

A SIMULATOR OF SATELLITE ATTITUDE DYNAMICS

[†] **Pedro Tavares, Bruno Sousa,** [‡] **Pedro Lima**

*Instituto de Sistemas e Robótica, pólo do Instituto Superior Técnico
Torre Norte, Av. Rovisco Pais, 1 - 1096 Lisboa Codex
Fax: (+351 1) 8418291 E-mail: [†] pts@isr.ist.utl.pt, [‡] pal@isr.ist.utl.pt*

Abstract: This article describes a simulator of small satellite attitude environment and dynamics, complete with a set of realistic sensors and the most commonly used actuator in this class of satellites. The simulator described is useful in attitude estimation and control algorithm development. Some results of the simulation of the PoSAT-1 satellite are presented.

Keywords: simulators, satellite control, attitude, dynamics, sensors, magnetic field computation.

LIST OF SYMBOLS

The following symbols were used in this article¹:

<p>I moment of inertia matrix</p> <p>${}^S \Omega_{SI}(t)$ angular momentum vector of the SCS relative to the ICS expressed in the SCS</p> <p>${}^S N_{ctrl}(t)$ control torque expressed in the SCS</p> <p>${}^S N_{gg}(t)$ gravity gradient torque expressed in the SCS</p> <p>${}^S m(t)$ magnetic moment</p> <p>n_{coil} number of turns of the coil</p> <p>$i_{coil}(t)$ coil current</p> <p>A_{coil} area of the coil</p> <p>μ Earth's gravitational constant</p> <p>R_{CM} distance from the satellite's centre of mass to the Earth's centre of mass.</p> <p>q attitude quaternion</p> <p>q_4 fourth scalar component of the attitude quaternion</p> <p>ω_0 satellite's orbital angular velocity</p> <p>M mean anomaly</p> <p>E eccentric anomaly</p> <p>e eccentricity</p>	<p>ν true anomaly</p> <p>r distance to Earth's centre-of-mass (CM)</p> <p>a semimajor axis of the orbit</p> <p>n mean motion</p> <p>${}^S n_{coil}$ unit vector orthogonal to the coil plane</p> <p>T_{orbit} orbital period</p> <p>ω argument of perigee</p> <p>Ω longitude of the ascending node</p> <p>i inclination of the orbit</p> <p>${}^i X, {}^i Y, {}^i Z$ position of the satellite in the orbital plane</p> <p>r geocentric distance</p> <p>θ coelevation</p> <p>ϕ East longitude from Greenwich</p> <p>a equatorial radius (6371.2 Km adopted for the <i>International Geomagnetic Reference Field - IGRF</i>)</p> <p>$V(r, \theta, \phi)$ potential function</p> <p>P_n^m Schmidt normalised Legendre functions</p> <p>$P^{n,m}$ Gauss normalised Legendre functions</p> <p>g_n^m, h_n^m (Schmidt normalised) gaussian coefficients</p> <p>$g^{n,m}, h^{n,m}$ (Gauss normalised) gaussian coefficients</p> <p>B Earth's geomagnetic field</p> <p>B_i, B_j, B_k components of B in the LHCS</p>
--	--

¹ This work was supported by PRAXIS XXI program project PRAXIS/3/3.1/CTAE/1942/95

1 INTRODUCTION

The trade-off between space, power and weight available and the price tag and level of risk considered acceptable, is making small satellites increasingly popular. Their relative low cost and fast turn-around time (from contract to launch) make them a satisfactory means of access to space, not only for universities and small nations, but also for major players like ESA and NASA.

A core system for most satellites, whether big or small, is the Attitude Determination and Control System (ADCS), that enables the pointing of the satellite, or the stabilisation of its rotation. In micro-satellites the ADCS is affected by the same trade-offs as the other systems, resulting in less powerful sensors and actuators due to cost and size/weight criteria. Hence there is the need for adequate control strategies that take this trade-off into account. The need for a simulation tool to test and enable comparison of such strategies is obvious and thus the work summarised here, on the development of a satellite attitude dynamics simulator (Sousa, 1997).

The developed simulator reproduces the environment as perceived by the ADCS by modelling all quantities sensed or interacted with. Typical attitude sensors include Sun, Earth Horizon and Magnetic Field Sensors. Since small-satellites are typically in Low Earth Orbit (LEO), the preferred attitude actuators are those which generate a magnetic momentum that interacts with Earth's geomagnetic field, thus generating a momentum that rotates the satellite. Small gas jets are also becoming an option for this class of satellites.

The simulator presented here is generic, enabling the users to make up a small satellite configuration from a set of existing sensors and actuators. This added flexibility allows the study of different ADCS scenarios and the study of the cost/quality relation when choosing sensors and actuators for a new mission.

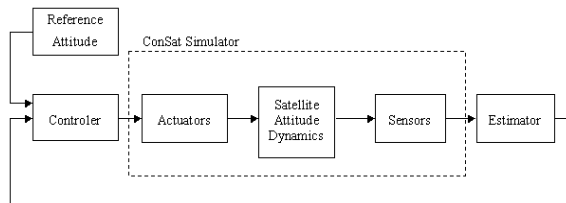


Fig. 1- ADCS Loop

2 SIMULATOR STRUCTURE

The *ConSat* simulator described in this paper simulates the environment as it is perceived and interacted upon by a small-satellite's ADCS (see

Fig. 1). The sensors' and actuators' model blocks are combined with a user-defined attitude determination and control algorithm block, using Simulink, and the output of the simulation is simultaneously saved to file and presented to the user using the simulator's graphical interface (see Fig. 2).

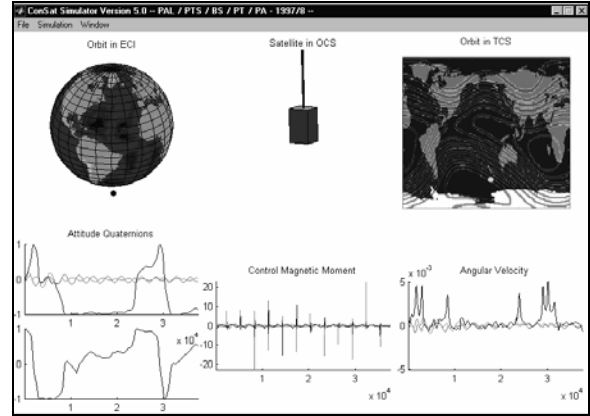


Fig. 2- *ConSat* Simulator Graphical Interface

The configuration parameters of each satellite (or case study for the simulator) are kept in a separate file, allowing an increased flexibility of the simulator's use.

3 MODELS

To simulate the evolution of the satellite attitude motion and the time-varying behaviour of all the sensors, several models had to be implemented, as depicted in Fig. 3.

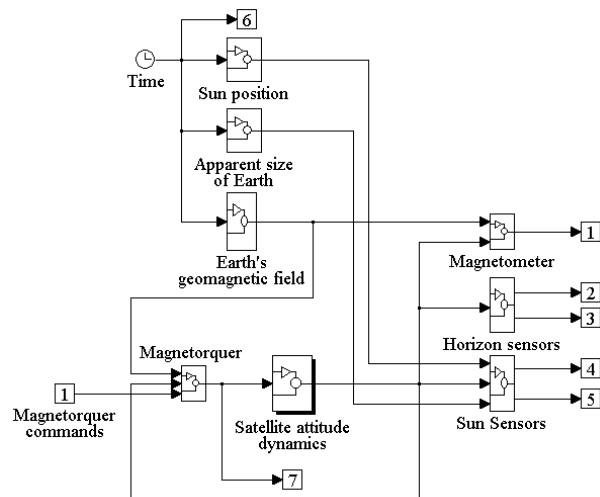


Fig. 3 - *ConSat* Simulator Block Diagram

The attitude motion of the satellite is modelled by the Euler equations for the motion of a rigid body under the influence of external moments, such as the control moment generated by the actuator. The

simulation of the actuator (a magnetorquer) requires the use of a geomagnetic field model and the calculation of the satellite position using an orbit model.

The sensors modelled are a 3-axis magnetometer, two single-axis Earth horizon sensors and two single-axis Sun sensors. The simulation of these sensors requires the knowledge of the magnetic field vector (for the magnetometer) and of the position of the Sun and Earth as seen from the satellite (for the Sun and Earth horizon sensor). One of the main control problems faced here is the fact that, besides being noisy, the information provided by the Sun and Earth sensors is not always available, depending on the relative positions of the satellite, Sun and Earth.

3.1 Dynamics and Kinematics

The Euler equations for the motion of a rigid body under the influence of external torques relate the rotational motion between an inertial reference coordinate system and another coordinate system, attached to the satellite.

The *Satellite Attitude Dynamics* block of Fig. 3 is expanded in Fig. 4:

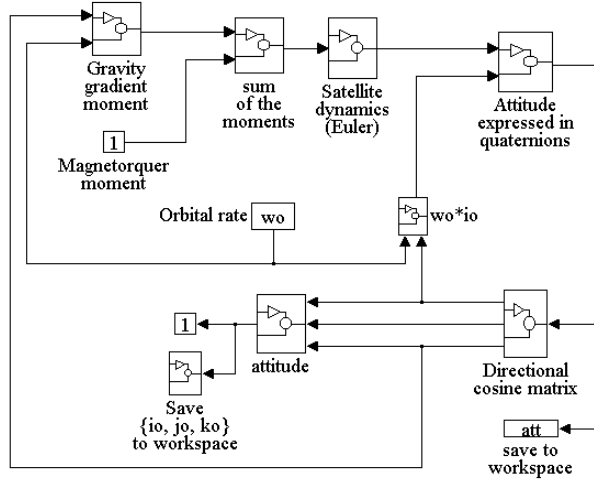


Fig. 4 - *Satellite Attitude Dynamics* Block Diagram

The three different reference coordinate systems (CS) employed in this attitude simulator are:

Inertial (ICS): $\{i_I, j_I, k_I\}$ is a right orthogonal CS centred on Earth's CM that is fixed (doesn't rotate with Earth). i_I is along the vernal equinox (1st point of Aries Υ , or the vector along the line passing Earth's and the Sun's CM on the last day of autumn, pointing away from the Sun). k_I is along the spin axis of the Earth and points from south to north and j_I complements this right orthogonal CS.

Terrestrial (TCS): $\{i_T, j_T, k_T\}$ is a right orthogonal CS centred on Earth's CM. It coincides with ICS on the vernal equinox and rotates with Earth.

Local Horizontal (LHCS): $\{i_{LH}, j_{LH}, k_{LH}\}$ is a right orthogonal CS centred in the CM of the satellite. i_{LH} is pointing along the Zenith, j_{LH} along East longitude and k_{LH} along South positive coelevation.

Orbital (OCS): $\{i_o, j_o, k_o\}$ is a right orthogonal CS centred in the CM of the satellite. i_o is orthogonal to the plane of the orbit (right-hand rule), k_o is pointing to the Zenith and j_o forms a right orthogonal system.

Satellite (SCS): $\{i_s, j_s, k_s\}$ is a right orthogonal CS centred in the centre of mass of the satellite, parallel to principal moment of inertia axle of satellite. k_o is parallel to the smallest moment of inertia axis (along gravity gradient boom, if present) and i_o and j_o are parallel to the two remaining principal moment of inertia of the satellite.

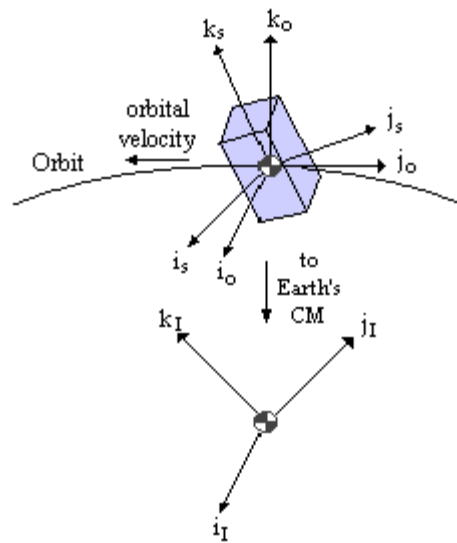


Fig. 5 - Inertial, Orbital and Satellite Coordinate Systems

The rigid body attitude dynamics, expressed in quaternions (Wisniewski, 1997) are:

$$I^S \dot{\mathcal{Q}}_{SI}(t) = -{}^S \Omega_{SI}(t) \times I^S \Omega_{SI}(t) + {}^S N_{ctrl}(t) + {}^S N_{gg}(t) \quad (1)$$

The kinematics of the satellite (*Quaternion representation of the satellite's attitude* block of Fig. 4) is:

$$\begin{aligned} \dot{q}_4 &= \frac{1}{2} {}^S \Omega_{SO} \cdot q_4 - \frac{1}{2} {}^S \Omega_{SO} \times q \\ \dot{q}_4 &= -\frac{1}{2} {}^S \Omega_{SO} \cdot q \end{aligned} \quad (2)$$

The relation between the satellite's and Earth's angular velocity is:

$${}^S \Omega_{SO} = {}^S \Omega_{SI} - \omega_0 \cdot {}^S i_O \quad (3)$$

3.2 ORBITAL MECHANICS

The orbit generator of this simulator uses the Kepler equation to calculate the position of the satellite's centre-of-mass in the ICS (Wertz, 1995).

$$\begin{aligned} {}^i X &= r \cdot [\cos(\omega + \nu) \cdot \cos(\Omega) - \sin(\omega + \nu) \cdot \sin(\Omega) \cdot \cos(i)] \\ {}^i Y &= r \cdot [\cos(\omega + \nu) \cdot \sin(\Omega) + \sin(\omega + \nu) \cdot \cos(\Omega) \cdot \cos(i)] \\ {}^i Z &= r \cdot [\sin(\omega + \nu) \cdot \sin(i)] \end{aligned} \quad (4)$$

Figure 6 shows 3 PoSAT orbits.

3.3 Geomagnetic Field Model

The *ConSat* simulator computes the Earth's geomagnetic field (EGF) B as the gradient of a scalar potential function V that is modelled by a series of spherical harmonics whose coefficients (g_n^m , h_n^m) are known for the IGRF (see Fig. 7).

$$B = -\nabla V \quad (5)$$

$$\begin{aligned} V(r, \theta, \phi) &= a \cdot \sum_{n=1}^k \left(\frac{a}{r}\right)^{n+1} \cdot \sum_{m=0}^n (g_n^m \cdot \cos(m \cdot \phi) + \\ & h_n^m \cdot \sin(m \cdot \phi)) P_n^m(\theta) \end{aligned} \quad (6)$$

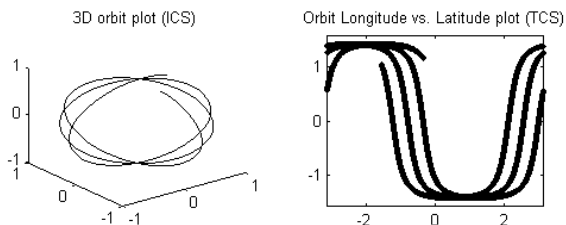


Fig. 6 - Three PoSAT-1 Orbits

To obtain increased computational efficiency the Legendre functions P_n^m are computed recursively

after being Gauss normalised. The resulting equations for EGF are then (Wertz, 1995):

$$\begin{aligned} B_i &= \frac{-\partial V}{\partial r} = \sum_{n=1}^k \left(\frac{a}{r}\right)^2 \cdot (n-1) \cdot \\ & \sum_{m=0}^n (g_n^m \cdot \cos(m \cdot \phi) + h_n^m \cdot \sin(m \cdot \phi)) \cdot \\ & P_n^m(\theta) \end{aligned} \quad (7)$$

$$\begin{aligned} B_j &= \frac{-1}{r \cdot \sin(\theta)} \cdot \frac{\partial V}{\partial \phi} = \frac{-1}{\sin(\theta)} \sum_{n=1}^k \left(\frac{a}{r}\right)^{n+2} \cdot \\ & \sum_{m=0}^n m \cdot (-g_n^m \cdot \sin(m \cdot \phi) + h_n^m \cdot \cos(m \cdot \phi)) \cdot \\ & P_n^m(\theta) \end{aligned} \quad (8)$$

$$\begin{aligned} B_k &= \frac{-1}{r} \cdot \frac{\partial V}{\partial \theta} = -\sum_{n=1}^k \left(\frac{a}{r}\right)^{n+2} \cdot \\ & \sum_{m=0}^n (g_n^m \cdot \cos(m \cdot \phi) + h_n^m \cdot \sin(m \cdot \phi)) \cdot \\ & \frac{\partial P_n^m(\theta)}{\partial \theta} \end{aligned} \quad (9)$$

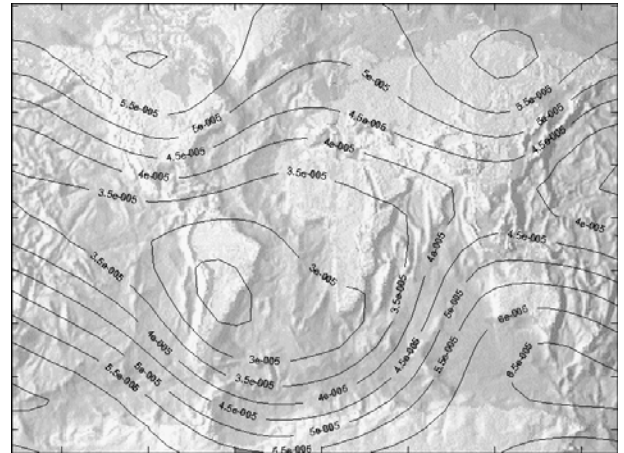


Fig. 7 - Earth's Geomagnetic Field - Simulation

4 VALIDATION: POSAT-1 CASE STUDY

To verify the simulator's usefulness a case study was used. The satellite chosen for this work was PoSAT-1, Portugal's first satellite (Ward, 1996), a technology demonstration satellite launched via Ariane from Kourou on September 26, 1993 on a 788×802 Km orbit at 98.7 degrees inclination (see Fig. 6).

This case study was used to make preliminary validation of the simulated data by comparison with real data. This comparison was made without determination of the satellite's attitude from the real

data² and thus, without simulating with the same initial values.

This chapter describes this satellite's sensors and actuator, showing real and simulated data for each sensor.

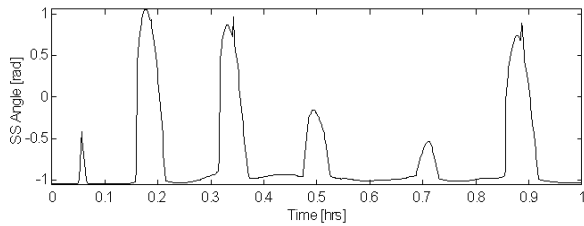


Fig. 8 – Sun Sensor – Real Data

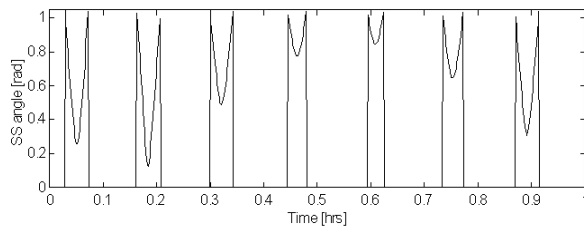


Fig. 9 – Sun Sensor – Simulated Data

4.1 PoSAT-1 Sensors

PoSAT-1 has two single-axis sun sensors, two single-axis Earth horizon sensors, two 3-axis magnetometers and an Earth underneath detector.

PoSAT-1's star sensor was not included in the simulation, since the data rate is too low for usage in a control loop (except for calibration purposes).

4.2 Sun Sensor

PoSAT-1's Sun sensors read the Sun angle to the sensor's axis whenever the Sun is inside that particular sensor's field-of-view. These sensors face the $-i$ and $-j$ axle. Real and simulated data, as well as a block diagram of the sensor, are plotted in Figures 8-10 showing a satisfactory resemblance despite the distinct initial conditions.

4.3 Earth Horizon Sensor.

PoSAT-1's Earth horizon sensors read the angle of Earth's horizon to the sensor's axis whenever the horizon is inside that particular sensor's field-of-view. These sensors also face the $-i$ and $-j$ axle. Real and simulated data, as well as a block diagram

² The attitude determination algorithm for PoSAT-1 of the ConSat simulator was not available at the time of print of this article.

of the sensor, are plotted in Figures 11-13. The real data shown has been previously filtered and processed to remove noise.

4.4 Magnetometers

PoSAT-1 has an internal and an external 3-axis fluxgate magnetometer. Real and simulated data are plotted in Figures 14 and 15 and show a good similarity.

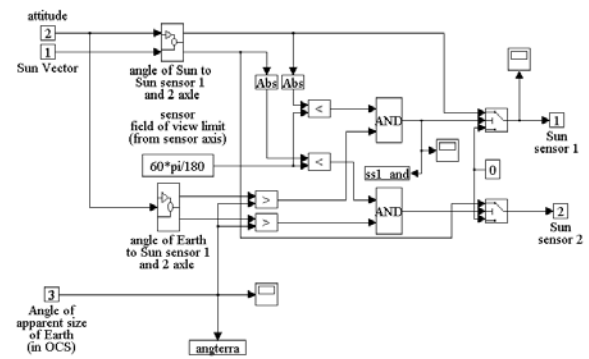


Fig. 10 – Sun Sensor – Block Diagram

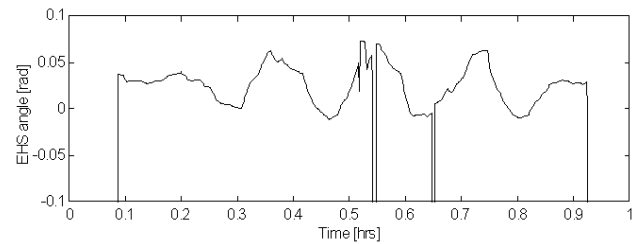


Fig. 11 – Earth Horizon Sensor – Real Data

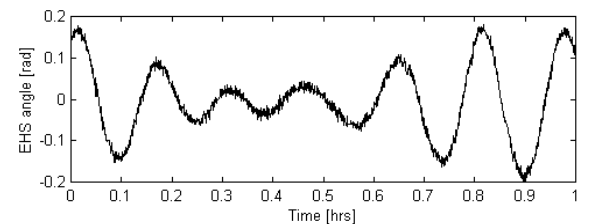


Fig. 12 – Earth Horizon Sensor – Simulated Data

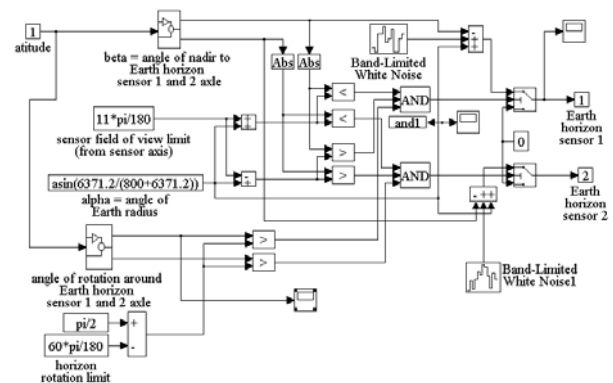


Fig. 13 – Earth Horizon Sensor – Block Diagram

5 CONCLUSIONS AND FUTURE WORK

This paper presented a simulator of small-satellite attitude dynamics, including the realistic simulation of magnetorquers and of sensor readings, with superimposed noise and data unavailability.

This simulator is currently being used to test attitude control algorithms. Preliminary results for the PoSAT-1 satellite show satisfactory similarities between real and simulated data, but further work must be done to calibrate the satellite model after implementation of the attitude estimation algorithm. Future work will also include the simulation of Ørsted, a Danish built satellite, as well as the inclusion of new sensor and actuator models.

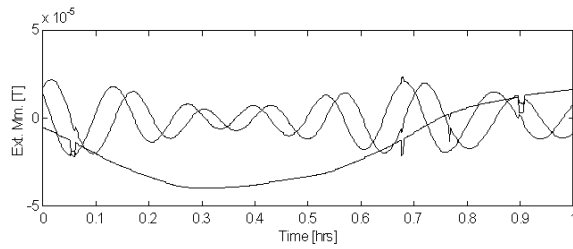


Fig. 14 – External Magnetometer – Real Data

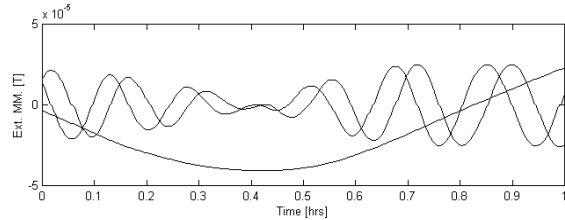


Fig. 15 – External Magnetometer – Simulated Data

4.5 PoSAT-1 Actuators

PoSAT-1 is stabilised with the help of a passive gravity gradient boom that generates a stabilising moment (Wertz, 1995):

$${}^S N_{gg} = \frac{3 \cdot \mu}{R_{CM}^3} \cdot ({}^S k_O \times I \cdot {}^S k_O) \quad (10)$$

The only (active) actuator present in this satellite is a magnetic torquer, which generates a magnetic moment that interacts with Earth's geomagnetic field, creating a moment to damp the libration motion around one of the satellite's attitude equilibrium points $k_s = \pm k_o$ (assuming $I_k \ll I_b, I_j$). The control moment generated is:

$${}^S N_{ctrl}(t) = {}^S m(t) \times {}^S B(t) \quad (11)$$

where the magnetic moment generated by the satellite's various coils is given by (Tavares, 1995):

$${}^S m(t) = \sum_{coil=1}^6 n_{coil} \cdot i_{coil}(t) \cdot A_{coil} \cdot {}^S n_{coil} \quad (12)$$

On PoSAT-1, $n_{coil,i-j} = 100$, $n_{coil,k} = 200$ and $A_{coil} = 0.11 \text{ [m}^2\text{]}$

ACKNOWLEDGEMENTS

The ESF COSY Programme supported some of the work presented in this article. The authors would also like to acknowledge the support of INETI and Marconi.

BIBLIOGRAPHY

- Sousa, Bruno. (1997). *Simulador da Dinâmica de Atitude de Micro-Satélites*. TFC, Instituto Superior Técnico.
- Tavares, Pedro. (1995). *Estimação e Controlo de Atitude de um Micro-Satélite*. TFC, DEEC, Instituto Superior Técnico.
- Ward, Jeffrey W., Price, Harold E. (1996). PoSAT-1. In: Wertz, James R., Larson, Wiley J., *Reducing Space Mission Cost*, Space Technology Library.
- Wertz, James R., (1995). *Spacecraft Attitude Determination and Control*, Kluwer Academic Publishers.
- Wisniewski, Rafal (1997), *Satellite Attitude Control Using Only Electromagnetic Actuation*, Ph.D. Thesis, Dept. of Control Engineering, Aalborg University.